STAFF Spectrum Analyser

Treatment of the Calibration and Housekeeping Data

C.C. Harvey, F. Wouters,
Y. de Conchy, Lucien Sitruk

Bars indicate changes since Issue 5, Rev. 0, dated February 1, 1999

Contents

List of Figures

Appendices

1. Cross-references to Technical Note OBSPM–TN–0001
2. Determination of the Phase Calibration
3. Diagonalisation of a Hermitian matrix

Document Status Sheet

1. Document Title: **STAFF-SA Calibration and Housekeeping**

2. Document Reference Number: **OBSPM–TN–0005**

3. Issue	4. Revision	5. Date	6. Reason for Change
draft	0	October 26 1994	First draft
2	0	December 2, 1994	Document version number is same as for document TN–0001
2	1	February 1, 1995	R^n replaced by H^n throughout A_i^{mn} replaced by R_i^{mn} throughout
2	2	March 22, 1995	Major correction of eqs. 18 and 24 Explanation after eq. 18
3	0	April 19, 1996	Start of major revision to take account of changes of Issue 4 of Paper TN-0001
3	1		Continuation
3	2		Continuation
3	3	April 23, 1996	Chaps. 1 through 3 brought under configuration control
3	4	April 29, 1996	New Sect. 4.4.2 concerning the phases of S_p^m and D_p^m. New Sect. 4.5 to take account of the sensor transfer functions. ρ_{ref} replaced by ρ^{ref} for editorial reasons. Additional explanation in Chap. 2. Re-definition of parameter α^{mn}. Clarification of the definition of $D_{Bs}^m(A_{\mathrm{ref}}^m)$ (eq. 23.
4	0	May 27 1996	Corrections to eqs. 35, 38 and 39
4	1	September 5, 1997	First version produced under UNIX
4	2	January 25, 1998	Missing parenthesis inserted in eq. 19 Reworded explanation of eq. 23 Extension of eqs. 24 to E_s
5	0	February 1, 1999	Source converted to LaTeX2 Major revision, change bars not used New first paragraph of Sect. 2 Substantial improvements to Sect. 3 Updated list of coefficients at end of Sect. 2 New Sect. 4.2 Substantial modifications to Sect. 4.4.2
5	1	February 16, 1999	Sects. entitled “Other relevant measurements” and “Description of the WEC housekeeping” removed. Sect. “Choice of three reference frequencies” deleted due to use of least squares method. Material moved from Sect. 4.4.2 to Sect. 3. Substantial clarification of Sect. 4.4.1. Quality factor W defined by eq.13 and used in Sect. 4.4.2. Completion of Sect. 4.4.2. Sect. 3.1 modified in accordance with the above. New Sect. 5

1 Introduction

This paper describes analysis of the engineering data from the STAFF Spectrum Analyser; this include the treatment of laboratory and in-flight calibration data, and of the housekeeping data. The instrument itself, and the calibration model are fully described in a companion document, ref. OBSPM–TN–0001.

There are numerous cross-references between these two documents, both of which are susceptible to revision. Accordingly, Appendix 1 of each document provides a table of cross-references between the documents. In this document, all references such as "eq. ref. n of Appendix 1" refer to an equation which occurs in the companion paper OBSPM–TN–0001. Its precise location can be found by referring to item # x in the Appendix 1 of paper OBSPM–TN–0001. Thus , it is possible to locate the desired equation, figure, section or chapter. Appendix 1 of each paper is derived by different processing of the same LaTeX file; this ensures that cross-references are handled systematically and consistently in the two papers.

2 The Calibration Model

As explained in Paper 1, the analytic signal X_i at the output of the analogue receiver operating in band m connected to input i may be expressed in terms of the analytic signal x_i at the input by eq. ref. 1 of Appendix 1), that is, (*Label* **ATF4**)

$$X_i = x_i \, F_i^m(f, A) + n_i^m(f) \; . \tag{1}$$

Here $F_i^m(f_n, A_i^m)$ is the analogue receiver transfer function, and $n_i^m(f)$ represents random noise from within the receiver. The transfer function $F_i^m(f_n, A_i^m)$ is complex and represents both the amplitude and the phase of the receiver transfer function. The noise signals $n_i^m(f_n)$ originating from different receivers (different values of m, i) are uncorrelated, and therefore the noise of each receiver is adequately described by its spectral power densities $< nn^* >_i^m (f_n)$. The purpose of the receiver calibration is to determine all the functions $F_i^m(f_n, A_i^m)$ and $< nn^* >_i^m (f_n)$.

It was shown in Chapter ref. 3 of Appendix 1 that the despin algorithm introduces an apparent "coupling" between the spin-plane field components if the transfer functions of the pairs of spin-plane receivers are not identical (in both amplitude and in phase). The effects of this coupling can be corrected. The equations required for this are enormously simplified if the spin-plane transfer functions are expressed in terms of the sum and difference functions (eq. ref. 4 of Appendix 1), (*Label* **defSD5**)

$$\left.\begin{array}{rclcrcl} \mathcal{S}_{Bs} &=& \frac{1}{2}\left(F_{By}+F_{Bz}\right) & \quad\text{and}\quad & \mathcal{S}_{Es} &=& \frac{1}{2}\left(F_{Ey}+F_{Ez}\right) \\ \mathcal{D}_{Bs} &=& \frac{1}{2}\left(F_{By}-F_{Bz}\right) & & \mathcal{D}_{Es} &=& \frac{1}{2}\left(F_{Ey}-F_{Ez}\right) \end{array}\right\} \; . \tag{2}$$

There are two parallel reasons for making this change of variable:

mathematical: the algebra is considerably simplified, essentially because it is the terms $\mathcal{D}$ which introduce the cross-coupling between the spin-plane outputs. This simplification is especially useful when solving the resulting eq. 5 below for $< \overline{x}_i \overline{x}_j^* >$.

physical: the $\mathcal{D}$ functions represent the lack of balance in each pair of spin-plane receivers.

- the $\mathcal{D}$ functions are negligible when the spin-plane transfer functions are well-balanced;

- even when this is not the case, their contribution to the cross-coupling is negligible when the integration time is nearly an integral number of half-spin periods.

Having introduced these functions, it is convenient to separate the variables of the four functions $\mathcal{S}_{Bs}$, $\mathcal{D}_{Bs}$, $\mathcal{S}_{Es}$, and $\mathcal{D}_{Es}$, rather than of the four functions F_{By}, F_{Bz}, F_{Ey}, and F_{Bz}. At the same time, as explained in Sect. ref. 6 of Appendix 1, it is convenient to include the bandpass characteristic H^n of the digital filter is this separation, thus (eq. ref. 7 of Appendix 1) (*Label* **defSSPs5**)

$$\left.\begin{aligned} \mathcal{S}_p^m(f_n, A_p^m) &= \frac{1}{H^n} S_p^m(A_p^m) \times \tilde{S}_p^m(f_n) \\ \mathcal{D}_p^m(f_n, A_p^m) &= \frac{1}{H^n} D_p^m(A_p^m) \times \tilde{D}_p^m(f_n) \; . \end{aligned}\right\} \text{ for } p = 1, 2 \tag{3}$$

Then putting (eq. ref. 8 of Appendix 1) (*Label* **defSSPa5**)

$$\mathcal{S}_{Bx} = F_{Bx}^m(f_n, A_{Bx}^m) \; , \quad S_{Bx} = Q_{Bx}^m(A_{Bx}^m) \; , \quad \tilde{S}_{Bx} = H^n P_{Bx}^m(f_n) \; , \tag{4}$$

we obtain the overall (analogue + digital) receiver response (eq. ref. 9 of Appendix 1)

$$N_{ij}^{mn} = S_p^m(A_p^m) \, S_q^{m*}(A_q^m) \, \tilde{S}_p^m(f_n) \, \tilde{S}_q^{m*}(f_n) \left(< \overline{x}_i \overline{x}_j^* > + \Delta_{ij}^{mn}(A_p^m) \right) \quad \text{(no sum over } p, q) \tag{5}$$

The matrix Δ_{ij}^{mn} is given by eq. ref. 10 of Appendix 1; it is a function of $\epsilon_p = \mathcal{D}_p / \mathcal{S}_p$ ($p = B_s$ and/or E_s), the spin phase at the start and the end of the data integration interval, and elements of the matrix $< \overline{x}_i \overline{x}_j^* >$. These are the equations which must be solved to obtain $< \overline{x}_i \overline{x}_j^* >$ from the information in the telemetry data stream. Here the subscripts $p(i)$ takes the values (eq. ref. 12 of Appendix 1) (*Label* **defpq**)

$$p(1) = B_x, \qquad p(2) = B_s, \qquad p(3) = B_s, \qquad p(4) = E_s, \qquad p(5) = E_s \tag{6}$$

with a similar expression for $q(j)$.

Physical significance can be attached to the different calibration parameters (see ref. 13 of Appendix 1):

- The mean spectral noise density in the overall pre-converter passband of analogue receiver m, as a function of the corresponding AGC output A_p^m (which is measured in telemetry counts) can be defined to be (*Label* **defSQ**)

$$\rho_p^m = \frac{1}{\left[S_p^m(A_p^m) \right]^2} \; ; \tag{7}$$

  the units of $S_p^m(A_p^m)$ are $\left[\text{nT Hz}^{-\frac{1}{2}} \right]^{-1}$ (or $\left[[\text{V/m}] \text{ Hz}^{-\frac{1}{2}} \right]^{-1}$ for the electric field). Note that an isotropic magnetic spectral density yields $A_{Bs} = A_{Bx}$ (and not $A_{Bs} = 2A_{Bx}$) when the axial and spin-plane receivers have identical gain.

- The mean spectral density of the axial field component in the frequency passband f_n of band m is then given by

$$\rho_p(f_n^m) = \frac{N_{ii}^{mn}}{\left| S_{Bx}^m(A_{Bx}^m) \; \tilde{S}_{Bx}^m(f_n) \right|^2} \; . \tag{8}$$

  The units of $\tilde{S}_{Bx}^m(f_n)$ are (telemetry counts)$^{\frac{1}{2}}$.

- The mean (in the frequency channel f_n) spin-plane power spectral density can be shown (in Sect. 4.3.3, eq. 25) to be

$$\rho_p(f_n^m) \;=\; \frac{N_{ii}^{mn} + N_{i+1,i+1}^{mn}}{\left| S_p^m(A_p^m)\, \tilde{S}_p^m(f_n) \right|^2} \qquad \text{for } i = 2 \text{ or } 4 \tag{9}$$

  where p is determined by eq. 6. Note that for isotropic noise, the mean (over the band of frequencies around f_n^m) spin-plane power density is twice the axial power density, as expected.

It is convenient to treat the internal noise signals in a similar way, so that (eq. ref. 5 of Appendix 1) (*Label* **defMN**)

$$\begin{aligned} \mathcal{N} &= \tfrac{1}{2}(< n_i n_i^* > + < n_k n_k^* >) \\ \mathcal{M} &= \tfrac{1}{2}(< n_i n_i^* > - < n_k n_k^* >) \end{aligned} \tag{10}$$

2.1 The Calibration Coefficients

The complete list of parameters required in this calibration model is given in Sect. ref. 14 of Appendix 1:

$S_{Bx}^m(A_{Bx}^m)$		are each $m \times A = 3 \times 256 = 768$ point tables,
$S_{Bs}^m(A_{Bs}^m)$	$D_{Bs}^m(A_{Bs}^m)$	yielding a total of $5 \times 768 = 3840$ complex values
$S_{Es}^m(A_{Es}^m)$	$D_{Es}^m(A_{Es}^m)$	(*i.e.*, 7680 real values)
$\tilde{S}_{Bx}^m(f_n)$		are each $m \times n = 3 \times 9 = 27$ point tables,
$\tilde{S}_{Bs}^m(f_n)$	$\tilde{D}_{Bs}^m(f_n)$	yielding a total of $5 \times 27 = 135$ complex values
$\tilde{S}_{Es}^m(f_n)$	$\tilde{D}_{Es}^m(f_n)$	(*i.e.*, 270 real values)
$\tilde{N}_{Bx}^m(f_n)$		are each $m \times n = 3 \times 9 = 27$ point tables,
$\tilde{N}_{Bs}^m(f_n)$	$\tilde{M}_{Bs}^m(f_n)$	yielding a total of $5 \times 27 = 135$ complex values
$\tilde{N}_{Es}^m(f_n)$	$\tilde{M}_{Es}^m(f_n)$	(*i.e.*, 270 real values)
$z_{ii}(p)$		is a 256 point table, or a mathematical expression, for the (real) diagonal elements
$z_{ij}(p)$		is a 256 point table, or a mathematical expression, for the (complex) non-diagonal elements.

If supplied entirely in tabular form, the total number of coefficients required for one calibration set (i.e., for one instrument at one time) is

$$7680 + 270 + 270 + 256 + 512 = 8988 \text{ real coefficients.}$$

It is the purpose of this document to explain how to determine the tables S, D, $\tilde{S}$, $\tilde{D}$, $\tilde{N}$ and $\tilde{M}$.

3 Determination of the Calibration Coefficients

In this section we show how the calibration coefficients listed in Section 2.1 can be calculated from physical measurements made with the STAFF-SA instrument in the laboratory. Practical details of how this is done are given in Technical Note TN-0006. During the mission these coefficients can be partially validated using data from the in-flight calibration cycle ; this is the subject of Technical Note TN-0007.

The determination of these calibration coefficients is complicated by the fact that they cannot be measured directly. All laboratory or in-flight measurements determine the individual receiver transfer functions $F_i^m(A_p^m, f_n)$. If it is assumed that

$$F_i^m(f_n, A_i^m) = P_i^m(f_n) \times Q_i^m(A_i^m), \tag{11}$$

(see Paper I, ref. 2 of Appendix 1), then it is seemingly rather easy to determine the variations of the functions P and Q :

1. By holding the AGC constant at some value $A_p^m = A_{p\,\mathrm{ref}}^m$ it is possible to determine the function $P_i^m(f_n)$, and

2. By examining one particular frequency $f_n = f_{\mathrm{ref}}^m$ while varying A_p^m it is possible to determine the function $Q_i^m(A_i^m)$.

The resulting function F_i^m determined from eq. 11 appears to describe the measurements rather well simply because that is how the measurements were performed : the variation with frequency was performed at constant A_p^m ref, and the variation of gain with AGC level was measured at constant frequency f_{ref}^m. But we do not know how well this function represents $F_i^m(f_n, A_i^m)$ when $A_p^m \neq A_{p\,\mathrm{ref}}^m$ and $f_n \neq f_{\mathrm{ref}}^m$: that is, over the major part of the (A_p^m, f_n)-plane.

The present calibration model uses for the spin-plane receivers the separation of variables defined by eq.3. This is mathematically different from the separation of variables of eq. 11. There is no à priori reason for one separation of variables or the other to yield a better model of the receiver characteristics. But the separation of eq.3 does the undeniable advantage of allowing an analytic solution of the calibration model, something which was never achieved using eq. 11.

The functions $Q_i^m(A_i^m)$, $Q_{i+1}^m(A_i^m)$, $P_i^m(f_n)$ and $P_{i+1}^m(f_n)$ for the spin-plane receivers are relatively easy to determine, but it is mathematically impossible to map these functions directly to the functions $S_p^m(A_p^m)$, $D_p^m(A_p^m)$, $\tilde{S}_p^m(f_n)$ and $\tilde{D}_p^m(f_n)$ required by the separation of eq. 3. Therefore the passage from $F_i^m(A_p^m, f_n)$ and $F_{i+1}^m(A_p^m, f_n)$ to $S_p^m(A_p^m, f_n)$ and $D_p^m(A_p^m, f_n)$ is performed by a least squares method (described in Section 4.4.1) which, unlike the determination of P and Q described by steps 1 and 2 above, uses data from all points of the (A_p^m, f_n)-plane to determine the calibration coefficients, including those of the axial (B_x) component, whose variables are separated as in eq. 11. The acquisition of the necessary data is described in Section 4.4.1.

3.1 Procedure

The procedure described in this section is complete in itself. But it is not necessarily unique. What was actually done to calibrate the Cluster-2 flight models is described in the document TN-06.

The determinations of the calibration parameters involves seven distinct steps, using eq. 6. All must be performed with the experiment internal numerical despin commanded OFF.

1. Use eq. 7 to determine the variation of the modulus of the receiver transfer function with input noise level, for both the axial and the spin-plane components. Since no phase determination is involved, this is equivalent to the determination of the analogue receiver gain. Note that for $p = 2$ and $p = 3$:

   - the signals applied to the two inputs of each spin-plane pair should be identical (as there is only one value $A^m_{p\,\mathrm{ref}}$, see Section 4.1) ;
   - this determination is used (at step 4 below) in the determination of the functions $\tilde{S}^m_p(f_n)$ and $\tilde{D}^m_p(f_n)$ (see Section 4.3.3) ;
   - nevertheless, this condition will be relaxed (at step 6 below), for reasons explained in Section 4.4.2.

2. Determine the internal noise spectral density parameters $\mathcal{M}$ and $\mathcal{N}$, as described in Section 4.2.

3. Decide the signal levels ρ^m_p (nine values, for $1 \leq m \leq 3$ and $1 \leq p \leq 3$) at which eq. 8 for the axial component, and eq. 9 for the spin-plane components, are to represent exactly the variation of the transfer function with frequency f_n $(0 \leq n \leq 8)$. If ρ $\mathrm{nT}^2\,\mathrm{Hz}^{-1}$ is the spectral density of the white noise, we denote the reference noise level(s) used for frequency calibration by $\rho^m_{p\,\mathrm{ref}}$, with the result of step 1 enabling a corresponding values $A^m_{p\,\mathrm{ref}}$ to be assigned for the AGC level. Note that for $p = 2$ and $p = 3$ the signals applied to the two inputs of each spin-plane pair should be identical (Section 4.3.1).

4. Using measurements made with signals of intensity $\rho^m_{p\,\mathrm{ref}}$, determine completely (Sections 4.3.2 and 4.3.3) the variation with frequency of the transfer functions: that is, determine the functions $\tilde{S}^m_i(f_n)$ and $\tilde{D}^m_i(f_n)$. These functions take into account :

   - at each of the nine frequencies f_n, the phase differences between the five input channels at the reference signal level $\rho_{p\,\mathrm{ref}}$, and also
   - the gain differences between the two members of each pair of spin-plane channels.

   Note that, because all interchannel phase differences are included in the functions $\tilde{S}^m_i(f_n)$ and $\tilde{D}^m_i(f_n)$ (and absolute phase is not measured), it is possible to set:

   - the functions $S^m_p(A^m_{p\,\mathrm{ref}})$ to be real (*i.e.*, at the reference signal level);
   - the axial functions $\tilde{S}^m_{Bx}(f_n)$ to be real for all $1 \leq m \leq 3$ and $0 \leq n \leq 8$.

   It is also convenient to set (eq. 23)

   - $DQ^m_p(A^m_{p\,\mathrm{ref}}) = S^m_p(A^m_{p\,\mathrm{ref}})$

5. By varying the signals ρ^m_p separately for different values of p as described in Section 4.4.2, determine the amplitude and (relative) phase of $F^m_i(A^m_p, f^m_n)$. This gives, for each physical receiver, **complete knowledge** of the variation of the transfer function with both A^m_p and f^m_n.

6. To complete the calibration model, it remains only to determine the phase of $S_p^m(A_p^m)$ and the complex value of $D_p^m(A_p^m)$ from the known functions F_i^m. As explained in Paper TN–01 (ref. 19 of Appendix 1) and Section 4.4.2 of this document, there is no unique way to separate the independent variables A_p^m and f_n of the gain functions $F_i^m(A_p^m, f_n)$, and the separation of variables of the present calibration model is that of eq. 3. The corresponding calibration coefficients describing the variation of S and D with A_p^m are determined by a least squares method.

   Note that although S_p^m and D_p^m are defined to be real (and equal, see step 4) at the reference levels $\rho_{p\,\mathrm{ref}}^m$, in general they will be complex (and different) at other levels.

7. Finally, the resulting calibration coefficients must be corrected for the effects of the sensor transfer functions (Section 4.5.

The above operations may be performed in any order provided, of course, that
- step 3 is performed before step 4, and
- step 7 is performed last.

Once the calibration parameters have been thus determined for each band m then, to *within the limits of experimental error* :

- at the reference signal levels defined by $\rho_{p\,\mathrm{ref}}^m$ or, equivalently, by the corresponding AGC levels $A_{p\,\mathrm{ref}}^m$, the variation with frequency f_n of the gains and relative phases is described completely ;

- at the reference frequencies $f_{n\,\mathrm{ref}}^m$ the variation of the gains and the relative phases with the three AGC signals A_p^m is described completely.

For all other values in the (A_p^m, f_n)-plane the receiver transfer functions are only as good as the validity of the hypothesis eq. 3 of the separation of variables.

Calibration of the STAFF-SA instrument is not simple ! In particular, at step 6 we will be forced to abandon the determination of $S_p^m(A_p^m)$ performed in step 1, despite the fact that the result has been used at step 4. This inconsistency is not serious, because the value of $S_p^m(A_p^m)$ obtained at step 6 is nearly identical to that obtained at step 1. *(This assertation needs to be confirmed.)* There is a more rigorous solution to this apparent inconsistency ; it is outlined under point 4 of Section 5 (page 20.

3.2 Analysis of the cross-spectral matrix

All phase calibration is performed by analysis of the output from the digital cross-spectrum analyser. The cross-spectrum analyser determines the phase differences between all pairs of inputs, thus yielding ${}^5C_2 = 10$ phase differences per cross-spectral matrix. Of course, only four of these phase differences are significant : we may conveniently take these to be the phase advance of the B_y, B_z, E_y, and E_z channels with respect to the B_x channel. To remove internal inconsistencies and reduce the 10 phase differences to only 4, the procedure proposed in this section should be used.

The procedure described here also provides a parameter which indicates the quality of the phase determination. This is possible because the phase information is very over-determined, thus permitting relatively good internal self-consistency checking. It is also very important, because each individual phase determination is inherently rather poor. To economise telemetry, the non-diagonal elements of the cross-spectral matrix are encoding into 8-bit words, using 4 bits for the real part (including sign), and 4 bits for the imaginary part. The distribution of the "telemetry bins" in complex space is described in the document TN-02, "The computation of the STAFF cross-correlation". The digitalisation error varies between approximately $\pm 5°$ close to $\phi = 0°$, $\pm 90°$ or $180°$, and approximately $\pm 10°$ close to $\phi = \pm 45°$ or $\pm 135°$.

We now explain the procedure. Suppose that **phase coherent** white noise of spectral intensity ρ is applied simultaneously to all five sensors. Then

$$< x_i x_j^* > = \text{ constant for all } i, j$$

and the resulting matrix N_{ij}^n is proportional to $(H^n)^2 F_i F_j^*$; for each frequency f_n,

$$N_{ij}^{mn} = \alpha^{mn} \left(H^n\right)^2 F_i F_j^* ,$$

where the α^{mn} are constants (one for each frequency). By "white" noise, we mean noise with a spectrum which is constant throughout the range of frequencies for which spectral calibration is being performed.

This matrix enables all the functions F_i and F_j to be determined, except for the constants α^{mn} which can be determined later. The diagonal elements N_{ij}^n of the matrix determine are proportional the modulus of F_i

$$|F_i^m| = \frac{1}{H^n} \sqrt{\frac{N_{ii}^{mn}}{\alpha^{mn}}}$$

To determine the "best" estimate of the 4 independent inter-channel phase differences from the 10 inter-channel phase differences represented by (the off-diagonal elements of) the complete 5×5 cross-spectral matrix N_{ij}^n, we proceed as follows. We normalise the off-diagonal matrix elements defined by eq. ref. 18 of Appendix 1 to form the Hermitian matrices Z_{ij}^{mn} in which, for each frequency m, n, (*Label* **defZ**)

$$Z_{ij} = \begin{pmatrix} 1 & z_{12} & z_{13} & z_{14} & z_{15} \\ z_{21} & 1 & z_{23} & z_{24} & z_{25} \\ z_{31} & z_{32} & 1 & z_{34} & z_{35} \\ z_{41} & z_{42} & z_{43} & 1 & z_{45} \\ z_{51} & z_{52} & z_{53} & z_{54} & 1 \end{pmatrix} \qquad \text{where} \qquad z_{ji} = z_{ij}^* \, . \tag{12}$$

The eigenvector corresponding to the largest eigenvalue will give the "least squares" best estimate of the relative phases of the five receivers, whilst the ratio of the largest eigenvalue to the sum of the eigenvalues (equal to the trace of the matrix),

$$\frac{\lambda^{(5)}}{\lambda^{(1)} + \lambda^{(2)} + \lambda^{(3)} + \lambda^{(4)} + \lambda^{(5)}} = \frac{\lambda^{(5)}}{5} ,$$

will indicate the significance of the result, that is, the ratio of the coherent signal to the uncorrelated random fluctuations due to receiver, digital and other experimental noise. It is convenient to define the quality factor

$$W = \frac{\lambda^{(5)} - 1}{4} \, . \tag{13}$$

Thus defined, W lies in the range $0 \leq W \leq 1$, these limits corresponding respectively to 0 % and 100 % correlation. The justification of these results is given in Appendix 2.

The relative phases are defined by the elements of the eigenvector corresponding to the largest eigenvalue of the matrix Z_{ij}. Let this eigenvector be

$$e_i^{(5)} = e_i$$

This eigenvector is normalised neither in magnitude nor in phase. In the case of identity of all the receivers and no noise in the measurements (this perfect case is impossible to achieve if only because of digital noise), the matrix Z_{ij} will be

$$Z_{ij} = 1 \quad \text{for all } i, j$$

with largest eigenvalue $e^{(5)} = 5$, and the corresponding normalised eigenvalue

$$e_i = \frac{1}{5}\,(1,\,1,\,1,\,1,\,1)\;;$$

and the other eigenvalues are all zero. In the general case, the elements e_i^{mn} of the eigenvector will be complex. It is convenient to normalise the eigenvector so that phase is measured with respect to the B_x component, thus

$$e_i = (1,\,e_2,\,e_3,\,e_4,\,e_5)\;. \tag{14}$$

Then the transfer functions F are given by, (*Label* **defalph**)

$$F_i^m(A_p^m, f_n) \;=\; \frac{1}{H^n}\sqrt{\frac{N_{ii}^{mn}}{\alpha^{mn}}}\,e_i^{mn} \quad \text{for a signal of spectral density } \rho \tag{15}$$

Apart from the constants α^{mn}, these are exact expressions, in amplitude and in phase, for the transfer function F_i corresponding to a signal of spectral density $\rho_{\rm ref}$.

To determine α^{mn}, we note that from eqs. 3, 4 and 15,

$$S_{Bx}^m(A_i^m)\,\tilde{S}_{Bx}^m(f_n) \;=\; H^n\mathcal{S}_{Bx}^m(f_n, A_i^m) \;=\; H^nF_{Bx}^m(f_n, A_{Bx}^m) \;=\; \sqrt{\frac{N_{ii}^{mn}}{\alpha^{mn}}}$$

(since we have set $e_1^{mn} = 1$). Comparing this with eq. 18, we obtain

$$\alpha^{mn} \;=\; \rho_{\rm ref}\;,$$

so that eq. 15 becomes (*Label* **alph**)

$$F_i^m(A_i^m, f_n) \;=\; \frac{1}{H^n}\sqrt{\frac{N_{ii}^{mn}}{\rho_p^m}}\,e_i^{mn}\;. \tag{16}$$

where, in view of eq. 14, the phase differences are measured with respect to the B_x channel.

In reality, to perform measurements in each band m, white noise will be applied simultaneously to the different sensors, with different spectral intensities :

- $\rho_{Bx\,\rm ref}^m$ $\rm nT^2\,Hz^{-1}$ on the axial sensor,
- $\rho_{Bs\,\rm ref}^m$ $\rm nT^2\,Hz^{-1}$ on both spin-plane magnetic sensors, and
- $\rho_{Es\,\rm ref}^m$ $\rm [V/m]^2\,Hz^{-1}$ on both spin-plane electric sensors

(see Sect. 4.3.1). These different signals must all be **phase coherent**. The resulting AGC signals for the band m are $A_{Bx\,\rm ref}^m$, $A_{Bs\,\rm ref}^m$ and $A_{Es\,\rm ref}^m$. In this case the matrix elements $< x_i x_j^* >$ are not constant for all i, j, but nevertheless the matrix (of eq. 12) obtained after normalisation by the diagonal elements is unchanged, as is eq. 16.

In Section 4.4.1 ρ_{Bx}^m, ρ_{Bs}^m and ρ_{Es}^m will be varied independently. Special care must then be taken to remember that the relative phase differences are all measured with respect to the B_x channel.

4 Step by Step Determination of the Coefficients

4.1 The magnitude of $S_p^m(A_p^m)$

Suppose that white noise of spectral intensity ρ nT^2 Hz^{-1} is applied either to the B_x magnetic sensor, or simultaneously to the B_y and B_z magnetic sensors, or simultaneously to the E_y and E_z electric sensors, or any or all of these sensors, and let the resulting AGC signals A_{Bx}^m and/or A_{Bs}^m and/or A_{Es}^m be measured. The magnitude of the functions S_{Bx}^m and S_{Bs}^m are then defined by eq. 7 (*c.f.*, eq. ref. 15 of Appendix 1) (*Label* **defSQ5**)

$$\left|S_p^m(A_p^m)\right| = \rho^{-\frac{1}{2}} . \tag{17}$$

Note that there is a phase factor to be included in the coefficients $S_p^m(A_p^m)$ for $A_p^m \neq A_{p\,\mathrm{ref}}^m$. In Section 4.4.2 it will be shown how to determine these phase factors ; and it will also be shown that, to do this, the condition 17 has to be relaxed for $p = 2$ and 3, but in a way that has negligible practical consequences.

4.2 Determination of $\mathcal{M}_p^m$ and $\mathcal{N}_p^m$ (and of $|F_i^m|$, $\left|F_j^m\right|$) for $p = 2, 3$

Fig. 1 shows schematically the outputs X_i^m and X_j^m respectively from the E_i^m (or B_i^m, curve A) and E_j^m (or B_j^m, curve B) receiver outputs as functions of the input x_i^m while the x_j^m input is connected to a 50 Ω dummy load. The abscissa x_i^m is expressed in dB below the reference level ; thus small signals, corresponding to large receiver gains, occur to the right of the figure. Curve C shows the corresponding AGC output.

The X_i^m output is nearly constant (even on the real figures), showing that the AGC control is tight. The ratio of the output to input signal amplitude defines the magnitude of the gain. Thus the product "curve A $\times$ abscissa" (after appropriate corrections for the logarithmic compression of X_i^m and the logarithmic scale used for x_i^m) defines $\left|F_i^m(A_p)\right|$.

By interchanging the i and j inputs, that is, varying the x_j^m input signal while the x_i^m input is connected to a 50 Ω load, it is possible to determine $\left|F_j^m(A_p)\right|$.

For low values of the gain (left side of the figure), the X_j^m output is dominated by the post-AGC receiver noise and is nearly constant. The value of this constant determines the term $n_i^m(f)$ in eq. 1. The corresponding curve obtained after interchanging the i and j inputs allows the noise term $n_j^m(f)$ to be determined. Substitution of these values into eq. 10 yields $\mathcal{M}_p^m$ and $\mathcal{N}_p^m$.

It is not possible to use eq. 2 to determine $\left|D_p^m\right|$, because the relative phases are not known ; they are determined in Section 4.4.1. (Note that $\left|S_p^m\right|$ has already been determined in Section 4.1.)

Returning to the figure, for high values of the gain (right side of the figure), the X_j^m output increases as the gain increases. The slope of this part of the curve C defines the instrument sensitivity :

$$\frac{\partial X_j}{\partial A_p^m} = s_j^m \frac{\partial F_j^m(A_p^m)}{\partial A_p^m} = s_j^m F_j'^{\,m}(A_p^m)$$

where s_j^m is the receiver sensitivity of the input j of band m and $F_k'^{\,m}(A_p^m)$ can be determined from $F_j^m(A_p^m)$. Similarly, using measurements made varying x_j^m while x_i^m is connected to a dummy load, the sensitivity s_j^m can be determined.

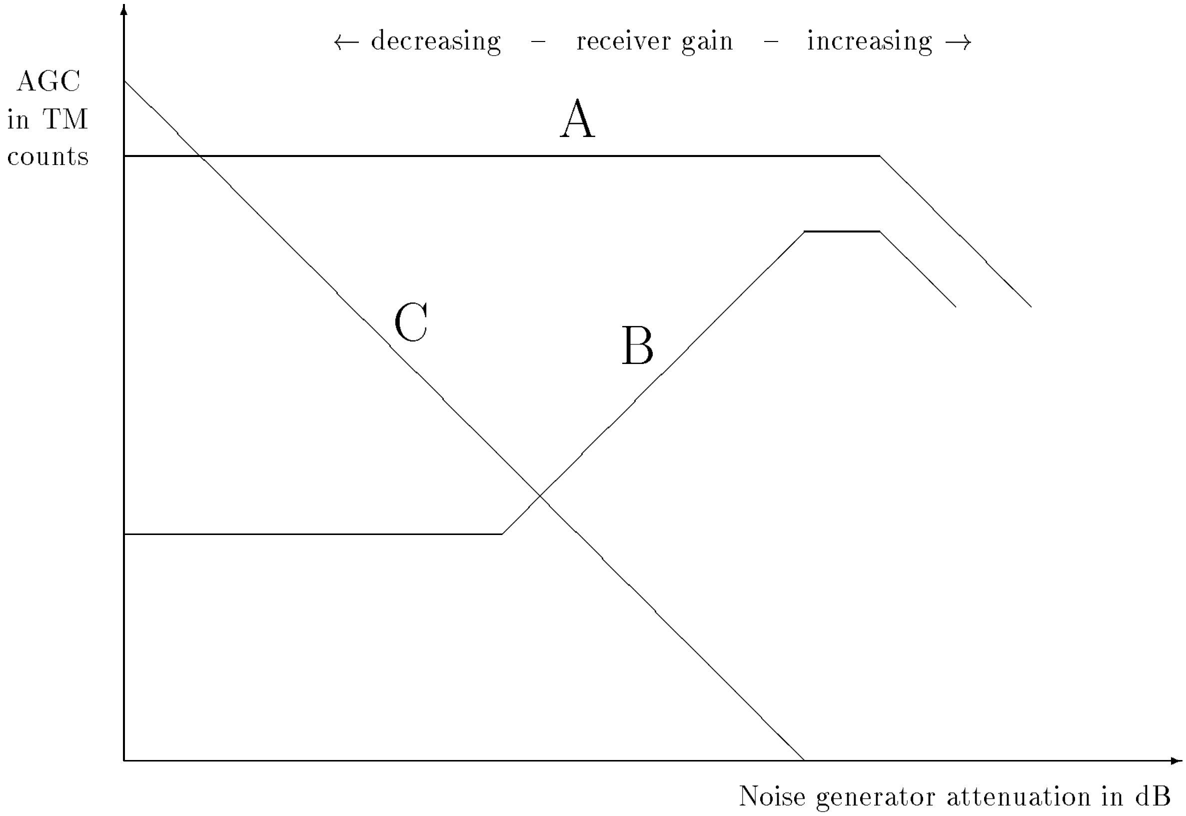

Figure 1: This figure shows schematically (curves A and B) how the analogue waveform outputs from a strapped pair of spin-plane receivers vary as the input to receiver A changes while the input to receiver B is connected to a $50\,\Omega$ dummy load. The two output signals are measured by the auto-correlation outputs of the digital spectrum analyser, and are expressed in telemetry counts. The abscissa is the input signal applied to input A, expressed in dB below the reference level; thus, high receiver gain occurs for small input signals, to the right of the figure. Curve C represents the AGC output (common to the two spin-plane receivers), likewise in telemetry counts.

Note that the spectral variation of the receiver noise represented by $\mathcal{M}$ and $\mathcal{N}$ (the noise due to n_i in eq. 17 of Paper 1) is different from that of the input noise which determines the overall receiver sensitivity.

4.3 Determination of the Variation with Frequency

4.3.1 Choice of the nine reference input noise levels $\rho^m_{p\,\mathrm{ref}}$

The receiver frequency calibration is performed at fixed input signal level. If ρ $\mathrm{nT}^2\,\mathrm{Hz}^{-1}$ (or $[\mathrm{V/m}]^2\,\mathrm{Hz}^{-1}$) is the spectral density of the white noise at the receiver input, we denote the reference noise level used for frequency calibration of band m by $\rho^m_{p\,\mathrm{ref}}$. This spectral density $\rho^m_{p\,\mathrm{ref}}$ will be situated at a value where the frequency variation of the transfer function changes only very slowly with signal amplitude. (If such a point does not exist, then the separation of variables expressed by eqs. 6 and 3 is invalid.) Normally this reference signal level will be somewhere near the middle of the receiver dynamic range. It should be at a signal level for which the quality parameter W_p^m (eq. 13 is good. Note that:

- Even if $\rho_{Bx\,\mathrm{ref}} = \rho_{Bs\,\mathrm{ref}}$, in general $A^m_{x\,\mathrm{ref}} \neq A^m_{Bs\,\mathrm{ref}}$.
- Conversely, if we choose $A^m_{Bx\,\mathrm{ref}} = A^m_{Bs\,\mathrm{ref}} = A^m_{Es\,\mathrm{ref}}$, then probably $\rho^m_{Bx\,\mathrm{ref}}$, $\rho^m_{Bs\,\mathrm{ref}}$ and $\rho^m_{Bs\,\mathrm{ref}}$ will all be different. This is certainly true for $\rho^m_{Es\,\mathrm{ref}}$: the electric field is of a different nature from the magnetic field.
- There is no reason for the reference signal levels to be always the same ; new calibration coefficients may be determined using different reference signal levels ; and the new set of coefficients will be perfectly compatible with the calibration model.

Further considerations to be taken into account when choosing the reference input noise levels are mentioned in Section 5.

4.3.2 The axial coefficient $\tilde{S}^m_{Bx}(f_n)$

To determine $\tilde{S}^m_{Bx}(f_n)$, we choose the reference spectral density $\rho^m_{Bx\,\mathrm{ref}}$ as described in Sect. 4.3.1. This will be the signal level at which the separation of variables of eq. 3 represents the functions $\mathcal{S}$ and $\mathcal{D}$ exactly for all values of f_n. The magnitude of the coefficient $\tilde{S}^m_{Bx}(f_n)$ is then defined by eqs. 8 and 7, thus (*Label* **defPx**)

$$\tilde{S}^m_{Bx}(f_n) = \frac{1}{|S^m_{Bx}(A^m_{Bx\,\mathrm{ref}})|}\sqrt{\frac{N^{mn}_{BxBx}}{\rho}} = \sqrt{N^{mn}_{BxBx}} \quad \text{for white noise input of density } \rho^m_{Bx\,\mathrm{ref}}\ . \tag{18}$$

$\tilde{S}^m_{Bx}(f_n)$ relates the output of the digital spectrum analyser at frequency channel n of band m to the white noise of spectral density $\rho^m_{Bx\,\mathrm{ref}}$ applied to the analogue receiver of band m; it has units of counts$^{\frac{1}{2}}$. For further details, see Paper I, esp. section 6.2.

The axial component is particularly simple because

- the functions $\tilde{S}^m_{Bx}(f_n)$ may be defined to be real (*c.f.* the normalisation of eq. 14), and
- the functions $D^m_{Bx}(A^m)$ and $\tilde{D}^m_{Bx}(f_n)$ do not exist.

When we examine the spin plane components, it is necessary to consider not only their relative phases between themselves, but also their phases relative to the axial component, as will now be explained.

4.3.3 The spin-plane coefficients $\tilde{S}^m_p(f_n)$ and $\tilde{D}^m_p(f_n)$

When the same signal is applied simultaneously to a pair of spin-plane sensors, in general the same values of the numerical output will not be obtained from the two corresponding analyser channels; for example, in eq. 9, $N^{mn}_{ByBy} \neq N^{mn}_{BzBz}$. To determine the calibration coefficients in this case, it is necessary to analyse the complete cross-spectral matrix.

When the despin is turned OFF, the cross-spectral matrix is related to the fields at the input to the receiver by eqs. ref. 16 of Appendix 1 and ref. 17 of Appendix 1, (*Label* **x2oX5**)

$$N^n_{ij} = (H^n)^2 < \overline{X}_i \overline{X}^*_j > = (H^n)^2 \, F_i F^*_j < x_i x^*_j > \tag{19}$$

The exact expressions for the spin-plane transfer functions are obtained as follows. From eqs. 2, 3 and 16

$$\left.\begin{aligned} S^m_{Bs}(A^m_{Bs\,\mathrm{ref}})\tilde{S}^m_{Bs}(f_n) &= \frac{1}{2}\left[\rho^m_{Bs\,\mathrm{ref}}\right]^{-\frac{1}{2}} \left(\sqrt{N^{mn}_{22}}\, e^{mn}_2 + \sqrt{N^{mn}_{33}}\, e^{mn}_3\right) \\ D^m_{Bs}(A^m_{Bs\,\mathrm{ref}})\tilde{D}^m_{Bs}(f_n) &= \frac{1}{2}\left[\rho^m_{Bs\,\mathrm{ref}}\right]^{-\frac{1}{2}} \left(\sqrt{N^{mn}_{22}}\, e^{mn}_2 - \sqrt{N^{mn}_{33}}\, e^{mn}_3\right) \end{aligned}\right\} \text{ for input noise } \rho^m_{Bs\,\mathrm{ref}} \tag{20}$$

with an equivalent pair of equations (involving N^{mn}_{44}, N^{mn}_{55}) and $\rho^m_{Bs\,\mathrm{ref}}$ for the spin-plane electric field. We arbitrarily put (but see discussion of Sect. 4.4.2)

$$\mathcal{I}m\{S^m_{Bs}(A^m_{Bs\,\mathrm{ref}})\} = 0 \tag{21}$$

because at the reference level $\rho^m_{p\,\mathrm{ref}}$ the inter-channel phase differences can be entirely described by $\tilde{S}$ and $\tilde{D}$.

So far we have not discussed $D^m_p(A^m_p)$ and $\tilde{D}^m_p(f_n)$. Like $S^m_p(A^m_p)$ and $\tilde{S}^m_p(f_n)$, they are defined by eq. 3. From eqs. 2 and 3,

$$\begin{aligned} F_{By} &= \mathcal{S}_{Bs} + \mathcal{D}_{Bs} = \frac{1}{H^n}\left[\, S^m_p(A^m_p) \times \tilde{S}^m_p(f_n) \;+\; D^m_p(A^m_p) \times \tilde{D}^m_p(f_n) \,\right] \\ F_{Bz} &= \mathcal{S}_{Bs} - \mathcal{D}_{Bs} = \frac{1}{H^n}\left[\, S^m_p(A^m_p) \times \tilde{S}^m_p(f_n) \;-\; D^m_p(A^m_p) \times \tilde{D}^m_p(f_n) \,\right] . \end{aligned} \tag{22}$$

While the magnitude of $S^m_{Bs}(A^m_{Bs})$ is determined (by eq. 17) so as to satisfy eq. 7, there is no clear physical meaning to be attached to the value of $D^m_p(A^m_p)$: it is merely a parameter in the calibration model which describes the relative variation of the difference $\mathcal{D}^m_p(f_n, A^m_p)$ with A^m_p; whatever value we assign to $D^m_p(A^m_p)$ at the reference level $A^m_p = A^m_{p\,\mathrm{ref}}$, the actual value of the difference $\mathcal{D}^m_p(f_n, A^m_{p\,\mathrm{ref}})$ will be determined by $\tilde{D}^m_p(f_n)$. Therefore it is convenient to define (see again Sect. 4.4.2) (*Label* **modDQ**)

$$D^m_{Bs}(A^m_{Bs\,\mathrm{ref}}) = S^m_{Bs}(A^m_{Bs\,\mathrm{ref}}) \tag{23}$$

so that, using eq. 17, (*Label* **defSDP**)

$$\left.\begin{aligned} \tilde{S}^m_{Bs}(f_n) &= \tfrac{1}{2}\,(\sqrt{N^{mn}_{22}}\, e_2 + \sqrt{N^{mn}_{33}}\, e_3) \\ \tilde{D}^m_{Bs}(f_n) &= \tfrac{1}{2}\,(\sqrt{N^{mn}_{22}}\, e_2 - \sqrt{N^{mn}_{33}}\, e_3) \end{aligned}\right\} \text{ for input noise density } \rho^m_{Bs\,\mathrm{ref}}\,, \tag{24}$$

with an equivalent pair of equations (involving N^{mn}_{44} and N^{mn}_{55}) for $\tilde{S}^m_{Es}(f_n)$ and $\tilde{D}^m_{Es}(f_n)$.

For values $A^m_p \neq A^m_{p\,\mathrm{ref}}$, in general $D^m_p(A^m_p) \neq S^m_p(A^m_p)$, because D^m_p and S^m_p take account of the variation of F with AGC level ; their determination is described in Section 4.4.2.

Eq. 23 applies only for for $A^m_p = A^m_{p\,\mathrm{ref}}$, and is introduced solely for the purpose of defining values for $\tilde{S}^m_{Bs}(f_n)$ and $\tilde{D}^m_{Bs}(f_n)$ via eq. 24. Once $\tilde{S}^m_{Bs}(f_n)$ and $\tilde{D}^m_{Bs}(f_n)$ have been thus determined, then for $A^m_{Bs} \neq A^m_{Bs\,\mathrm{ref}}$ the (complex) value of $D^m_p(A^m_{Bs})$ and the phase of $S^m_{Bs}(A^m_{Bs})$ (the magnitude is fixed by eq. 7) must be determined as explained in Section 4.4.2.

Finally in this section, we note from eq. 3 and from eq. ref. 27 of Appendix 1 that the total spin-plane power in the channel n of band m is (*Label* **defSPsc**)

$$\rho^m_p(f_n) = <\overline{x}_2\overline{x}^*_2> + <\overline{x}_3\overline{x}^*_3> = \frac{N^{mn}_{22} + N^{mn}_{33}}{\left|S^m_p(A^m_p)\ \tilde{S}^m_p(f_n)\right|^2} . \tag{25}$$

For an isotropic power spectrum the spin-plane power density is twice the axial power density (as expected).

Note that the contribution to the "partial trace" $< \overline{x}_2\overline{x}_2^* > + < \overline{x}_3\overline{x}_3^* >$ from the term Δ_{ij} in eq. ref. 27 of Appendix 1 can be shown to be zero; this can be seen from the equations of ref. 20 of Appendix 1. Therefore eq. 25 is exact. The the corresponding expressions for the separate components $< \overline{x}_2\overline{x}_2^* >$ and $< \overline{x}_3\overline{x}_3^* >$ require that Δ_{ij} be evaluated.

4.4 Determination of the Variation with AGC level

It remains to determine the phase of $S_p^m(A_p^m)$ and the complex value of $D_p^m(A_p^m)$ for $A_p^m \neq A_{p\,\mathrm{ref}}^m$. To do this, we explore the magnitude and relative phase of the functions $F_i^m(A_p^m, f_{\mathrm{ref}}^m)$ over the entire range of A_p^m and f_n^m (*i.e.*, everything which can be measured in the laboratory), and then fit the results to the calibration model using a least squares method. It turns out to be easier to do this if both the magnitude and the phase of $S_p^m(A_p^m)$ are determined, so as to treat $S_p^m(A_p^m)$ and $D_p^m(A_p^m)$ symmetrically. Thus the eq. 7 is relaxed for $p = 2$ and 3. The practical consequences are negligible.

4.4.1 The amplitude and relative phase of $F_i^m(A_p^m, f_n^m)$

The variation of the gain with frequency must be performed using a phase coherent signal, which may be either noise or sinusoidal, applied to all five entry channels.

Initially, the signal is applied with amplitude such that $A_p^m = A_{p\,\mathrm{ref}}^m$. As already mentioned, $A_{p\,\mathrm{ref}}^m$ need not be the same for all p (*i.e.*, it may have different values for B_x, B_s and E_s), but the signals applied to the inputs B_z and E_z should be the same as applied respectively to B_y and E_y. Generally, of course, $A_{p\,\mathrm{ref}}^m$ will also, have a different value for each band m.

Then, in turn, the different inputs are varied (say, in steps of 2 dB), causing one or other of A_{Bx}^m, A_{Bs}^m or A_{Es}^m to vary. At each step the analysis of Section 3.2 is performed to determine the four significant phase differences. Note that the amplitudes of each pair of spin-plane inputs must be varied together, because it is the larger of the two inputs which dominates the determination of the AGC level A_p^m.

Input varied	Parameters whose variation is determined
B_x	the magnitude and phase of $F_1^m(A_{Bx}^m, f_{n\,\mathrm{ref}}^m)$
B_y and B_z	the magnitude and phase of $F_2^m(A_{Bs}^m, f_{n\,\mathrm{ref}}^m)$ and $F_3^m(A_{Bs}^m, f_{n\,\mathrm{ref}}^m)$
E_y and E_z	the magnitude and phase of $F_4^m(A_{Es}^m, f_{n\,\mathrm{ref}}^m)$ and $F_5^m(A_{Es}^m, f_{n\,\mathrm{ref}}^m)$

These magnitudes and phases are determined as follows :

- For each frequency f_n, F_i^m is expressed in terms of its ratio R with respect to its value at the reference level $A_p = A_{p\,\mathrm{ref}}$,

$$F_i^m(A_p^m, f_n^m) = R_i^m(A_p^m, f_n^m) \times F_i^m(A_{p\,\mathrm{ref}}^m, f_n^m) \; . \tag{26}$$

- The magnitude of R is determined from the diagonal elements N_{ii} of the cross-spectral matrix with respect to their values at the reference level $\rho_{p\,\mathrm{ref}}$, thus

$$\left.\begin{array}{llllll} & & |R_1^m(A_{Bx}^m, f_n^m)| & = & \sqrt{\frac{N_{11}}{N_{11\,\mathrm{ref}}}\frac{\rho_{Bx\,\mathrm{ref}}}{\rho}} & \\ |R_2^m(A_{Bs}^m, f_n^m)| & = \sqrt{\frac{N_{22}}{N_{22\,\mathrm{ref}}}\frac{\rho_{Bs\,\mathrm{ref}}}{\rho}} & & |R_3^m(A_{Bs}^m, f_n^m)| & = & \sqrt{\frac{N_{33}}{N_{33\,\mathrm{ref}}}\frac{\rho_{Bs\,\mathrm{ref}}}{\rho}} \\ |R_4^m(A_{Es}^m, f_n^m)| & = \sqrt{\frac{N_{44}}{N_{44\,\mathrm{ref}}}\frac{\rho_{Es\,\mathrm{ref}}}{\rho}} & & |R_5^m(A_{Es}^m, f_n^m)| & = & \sqrt{\frac{N_{55}}{N_{55\,\mathrm{ref}}}\frac{\rho_{Es\,\mathrm{ref}}}{\rho}} \end{array}\right\} \tag{27}$$

- The phase of R is determined from the off-diagonal elements of the cross-spectral matrix. Eq.26 shows that the phase to be used is the difference between the phases measured at signal levels A_p^m and $A_{p\,\mathrm{ref}}^m$. As mentioned in Section 3.2, although the individual phases determined from the off-diagonal elements are somewhat imprecise, the fact there is redundancy in the phase measurements enables not only the precision to be improved, but also its quality $W_n^m(A_p^m)$ to be estimated (eq. 13, page 7) from the mutual consistency of the individual measurements. Since the phase does not vary rapidly with AGC level A_p^m, it is possible to plot the different phases against A_p^m and, by interpolation taking account of the quality $Q^m(A_p^m)$, obtain the variation of the phase with A_p^m with good precision.

- The method of Section 3.2 yields the four phases of F_{By}, F_{Bz}, F_{Ey} and F_{Ez} with respect to F_{Bx}. By definition, the phase F_{Bx} is zero at the reference level ρ_{ref} ; but in general it is not zero at other levels of ρ. When determining the phase of $F_{Bx}(\rho)$ with respect to $F_{Bx}(\rho_{\mathrm{ref}})$, it must be remembered that when ρ_{Bx} is varied it is the phases of F_{By}, F_{Bz}, F_{Ey} and F_{Ez} which are constant.

The determinations of the amplitude and phase of the different F_i^m can be compared with the determinations of $S_p^m(A_p^m)$ made in Sections 4.1, and more precisely but at the reference frequency $f_{n\,\mathrm{ref}}^m$ only, in Sections 4.3.2 and 4.3.3, and also the evaluation of F_i^m made in Section 4.2. It is assumed that these determinations agree within the limits of experimental error ; the method used to extract the "best values" of the magnitudes from these redundant determinations is described in the document TN–06.

4.4.2 The functions $D_p^m(A_p^m)$ and the phase of $S_p^m(A_p^m)$

The only calibrations parameters which remain to be determined are the functions $D_p^m(A_p^m)$ and the phase of $S_p^m(A_p^m)$. They must be determined from the functions F_i^m determined in Section 4.4.1. For this, we note that, using eq. 23, eqs. 22 may be expressed,

$$\begin{aligned}
\left[F_{By}(A_p^m) - F_{By}(A_{p\,\mathrm{ref}}^m)\right] H^n &= \\
&\left[S_p^m(A_p^m) - S_p^m(A_{p\,\mathrm{ref}}^m)\right] \tilde{S}_p^m(f_n) + \left[D_p^m(A_p^m) - D_p^m(A_{p\,\mathrm{ref}}^m)\right] \tilde{D}_p^m(f_n) \\
\left[F_{Bz}(A_p^m) - F_{Bz}(A_{p\,\mathrm{ref}}^m)\right] H^n &= \\
&\left[S_p^m(A_p^m) - S_p^m(A_{p\,\mathrm{ref}}^m)\right] \tilde{S}_p^m(f_n) - \left[D_p^m(A_p^m) - D_p^m(A_{p\,\mathrm{ref}}^m)\right] \tilde{D}_p^m(f_n)
\end{aligned} \tag{28}$$

where

$$\begin{aligned}
F_{By}(A_{p\,\mathrm{ref}}^m) &= \frac{1}{H^n} S_p^m(A_{p\,\mathrm{ref}}^m) \left[\tilde{S}_p^m(f_n) + \tilde{D}_p^m(f_n)\right] \\
F_{Bz}(A_{p\,\mathrm{ref}}^m) &= \frac{1}{H^n} S_p^m(A_{p\,\mathrm{ref}}^m) \left[\tilde{S}_p^m(f_n) - \tilde{D}_p^m(f_n)\right]
\end{aligned} \tag{29}$$

It can be seen how the different terms in eqs. 28 contribute to F_{By} and F_{Bz} as A_p (for $p = 2$ or 3) varies. When $A_p = A_{p\,\mathrm{ref}}$, all terms on the right of eqs. 28 are zero, and the variation with frequency of F_{By} and F_{Bz} is determined entirely by $\tilde{S}_p^m(f_n)$ and $\tilde{D}_p^m(f_n)$ via eq. 29 : indeed, this is how this is how $\tilde{S}_p^m$ and $\tilde{D}_p^m$ were defined in Section 4.3.3. As A_p departs from the value $A_{p\,\mathrm{ref}}$, so the contributions from the terms on the right of eqs. 28 increase.

As already mentioned (Section 3, page 4), there is no one-to-one mapping of the functions $F_i^m(A_p^m, f_n^m)$ to the functions $D_p^m(A_p^m)$ and the phase of $S_p^m(A_p^m)$. We note that the method of Section 4.4.1 determines the functions $F_i^m(A_p^m, f_n^m)$ over the whole of the (A_p^m, f_n^m)-plane ; the constraints of a separation of variables (*e.g.*, either eq. 3 or eq. 11) have not been imposed.

Therefore we use a method of least squares and the functions $F_i^m(A_p^m, f_n^m)$ over their entire domain of validity to derive the functions $D_p^m(A_p^m)$ and the phase of $S_p^m(A_p^m)$.

We note that :

1. $S_p^m(A_{p\,\mathrm{ref}}^m)$ has been arbitrarily made real (eq. 21), because any difference between the spin-plane transfer functions when $A_p^m = A_{p\,\mathrm{ref}}^m$ can be fully compensated by the parameters $\tilde{S}_p^m(f_n)$ and $\tilde{D}_p^m(f_n)$.
2. The magnitude of $S_p^m(A_p^m)$ has been defined by eq. 17, so as to provide useful function for estimating the broadband spectral density in physical units directly from the AGC signals.
3. The value of $D_p^m(A_{p\,\mathrm{ref}}^m)$ has been defined (by eq. 23) to be equal to $S_p^m(A_{p\,\mathrm{ref}}^m)$, so as to homogenise $\tilde{S}_p^m(f_n)$ and $\tilde{D}_p^m(f_n)$ (eqs. 24). Thus $D_p^m(A_{p\,\mathrm{ref}}^m)$ is real.

These points are noted in the order in which they could eventually be relaxed if it is found difficult to fit the model to the the functions F_i^m determined in Section 4.4.1. If they are all maintained, then the variation with AGC level A_p^m of all amplitudes and phase differences of between pairs of spin-plane channels must be described in terms of the complex value of $D_p^m(A_p^m)$ and the phase of $S_p^m(A_p^m)$ when $A_p^m \neq A_{p\,\mathrm{ref}}^m$.

In fact, it seems difficult to proceed without relaxing condition #2 on the above list.

Justification for relaxing condition #2

Eqs. 28 can be written

$$\begin{aligned} F_{By}(A) &= \left|S(A)\right|\tilde{S}(f_n)\, e^{i\,x(A)} + \tilde{D}(f_n)\, z(A) \\ F_{By}(A) &= \left|S(A)\right|\tilde{S}(f_n)\, e^{i\,x(A)} - \tilde{D}(f_n)\, z(A) \end{aligned}$$

where

$$\begin{array}{ccc} x(A) & \text{is a real function of} & A \\ z(A) & \text{is a complex function of} & A \end{array}$$

to be determined *(I am not sure that this exactly right, but it is not important for this discussion)*. It is difficult to solve these equations with the function x appearing in the exponent. It becomes much easier if we relax item #2 on the above list, so that these equations become

$$\begin{aligned} F_{By}(A) &= \tilde{S}(f_n)\, y(A) + \tilde{D}(f_n)\, z(A) \\ F_{By}(A) &= \tilde{S}(f_n)\, y(A) - \tilde{D}(f_n)\, z(A) \end{aligned}$$

where $y(A)$ and $z(A)$ are both complex functions of A, respectively (eq.3) S and D. The relaxation of the strict validity of eq. 17 (page 9) has negligible effect on its practical (approximate) validity of (unless the spin-plane receivers become very un- balanced).

The solution for $S_p^m(A_p^m)$ and $D_p^m(A_p^m)$

We can obtain a solution for the functions $S(A)$ and $D(A)$ by minimising, separately for each value of A, the sum of the residuals (*c.f.* eqs. 28 and 29)

$$\begin{aligned}\Sigma_{By} &= \sum_{n=0}^{8} W_n(A)\left|\tilde{S}(f_n)\,S(A)+\tilde{D}(f_n)\,D(A)-H^n F_{By}(A,f_n)\right|^2\\ \Sigma_{Bz} &= \sum_{n=0}^{8} W_n(A)\left|\tilde{S}(f_n)\,S(A)-\tilde{D}(f_n)\,D(A)-H^n F_{Bz}(A,f_n)\right|^2\end{aligned}$$

with respect to S and D. $W(A)$ is the quality factor of the phase determination, defined by eq. 13 (page 7). It can arbitrarily be put to zero, for example, to eliminate frequencies contaminated by interference (but see the discussion, Section 5).

To minimise the sum $\Sigma_{By}+\Sigma_{Bz}$ of the residuals, we put

$$\frac{\partial(\Sigma_{By}+\Sigma_{Bz})}{\partial S} = \frac{\partial(\Sigma_{By}+\Sigma_{Bz})}{\partial D} = 0\,,$$

which yields (using $\frac{\partial y^*}{\partial x} = (\frac{\partial y}{\partial x})^*$)

$$\begin{aligned}\sum_{n=0}^{8} W_n(A)\,\mathcal{R}e\Big\{&\left[\tilde{S}(f_n)\,S(A)+\tilde{D}(f_n)\,D(A)-H_n F_{By}(A,f_n)\right]\tilde{S}(f_n)^*\\ &+\left[\tilde{S}(f_n)\,S(A)-\tilde{D}(f_n)\,D(A)-H_n F_{Bz}(A,f_n)\right]\tilde{S}(f_n)^*\Big\} = 0\end{aligned}$$

$$\begin{aligned}\sum_{n=0}^{8} W_n(A)\,\mathcal{R}e\Big\{&\left[\tilde{S}(f_n)\,S(A)+\tilde{D}(f_n)\,D(A)-H_n F_{By}(A,f_n)\right]\tilde{D}(f_n)^*\\ &-\left[\tilde{S}(f_n)\,S(A)-\tilde{D}(f_n)\,D(A)-H_n F_{Bz}(A,f_n)\right]\tilde{D}(f_n)^*\Big\} = 0\,.\end{aligned}$$

We solve these equations separately for the real and the imaginary parts of $S(A)$ and $D(A)$, to obtain

$$S(A) = \frac{\sum_{n=0}^{8} W_n(A)\,H_n\left[F_{By}(A,f_n)+F_{Bz}(A,f_n)\right]\tilde{S}(f_n)^*}{2\,\sum_{n=0}^{8} W_n(A)\left|\tilde{S}(f_n)\right|^2}$$

$$D(A) = \frac{\sum_{n=0}^{8} W_n(A)\,H_n\left[F_{By}(A,f_n)-F_{Bz}(A,f_n)\right]\tilde{D}(f_n)^*}{2\,\sum_{n=0}^{8} W_n(A)\left|\tilde{D}(f_n)\right|^2}\,.$$

In full, these equations are

$$\left.\begin{aligned}S_{Bs}^m(A_{Bs}^m) &= \frac{\sum_{n=0}^{8} W_n^m(A)\,H_n^m\left[F_{By}^m(A_{Bs}^m,f_n^m)+F_{Bz}^m(A_{Bs}^m,f_n^m)\right]\tilde{S}_{Bs}^m(f_n^m)^*}{2\,\sum_{n=0}^{8} W_n^m(A)\left|\tilde{S}_{Bs}(f_n^m)\right|^2}\\ D_{Bs}^m(A_{Bs}^m) &= \frac{\sum_{n=0}^{8} W_n^m(A)\,H_n^m\left[F_{By}^m(A_{Bs}^m,f_n^m)-F_{Bz}^m(A_{Bs}^m,f_n^m)\right]\tilde{D}_{Bs}^m(f_n^m)^*}{2\,\sum_{n=0}^{8} W_n^m(A)\left|\tilde{D}_{Bs}(f_n^m)\right|^2}\,.\end{aligned}\right\}\quad(30)$$

These equations may be expressed in terms of the ratios R defined by eq. 26 which, together with eq. 29, gives

$$\begin{aligned}F_{By}^m(A_p^m,f_{n\,\mathrm{ref}}^m) &= R_{By}^m(A_p^m,f_{n\,\mathrm{ref}}^m)\times\frac{1}{H_n^m}\,S_p^m(A_{p\,\mathrm{ref}}^m)\left[\tilde{S}_p^m(f_n)+\tilde{D}_p^m(f_n)\right]\\ F_{Bz}^m(A_p^m,f_{n\,\mathrm{ref}}^m) &= R_{Bz}^m(A_p^m,f_{n\,\mathrm{ref}}^m)\times\frac{1}{H_n^m}\,S_p^m(A_{p\,\mathrm{ref}}^m)\left[\tilde{S}_p^m(f_n)-\tilde{D}_p^m(f_n)\right]\end{aligned}$$

so that

$$H_n^m \left[F_{By}^m(A_{Bs}^m, f_n^m) + F_{Bz}^m(A_{Bs}^m, f_n^m)\right] = S_{Bs}^m(A_{Bs\,\mathrm{ref}}^m)\left[R_{By}^m(A_{Bs}^m, f_n^m)\left(\tilde{S}_{Bs}^m(f_n) + \tilde{D}_p^m(f_n)\right) + R_{Bz}^m(A_{Bs}^m, f_n^m)\left(\tilde{S}_{Bs}^m(f_n) - \tilde{D}_p^m(f_n)\right)\right]$$

$$H_n^m \left[F_{By}^m(A_{Bs}^m, f_n^m) - F_{Bz}^m(A_{Bs}^m, f_n^m)\right] = S_{Bs}^m(A_{Bs\,\mathrm{ref}}^m)\left[R_{By}^m(A_{Bs}^m, f_n^m)\left(\tilde{S}_{Bs}^m(f_n) + \tilde{D}_p^m(f_n)\right) - R_{Bz}^m(A_{Bs}^m, f_n^m)\left(\tilde{S}_{Bs}^m(f_n) - \tilde{D}_p^m(f_n)\right)\right]$$

and finally

$$\begin{aligned} S_{Bs}^m(A_{Bs}^m) &= S_p^m(A_{p\,\mathrm{ref}}^m) \left\{\sum_{n=0}^{8} W_n^m(A)\left|\tilde{S}_{Bs}^m(f_n^m)\right|^2\right\}^{-1} \times \\ &\left\{\frac{1}{2}\sum_{n=0}^{8} W_n^m(A)\,\tilde{S}_{Bs}^m(f_n^m)^*\left[R_{By}^m(A_{Bs}^m, f_n^m)\tilde{E}_{22} + R_{Bz}^m(A_{Bs}^m, f_n^m)\tilde{E}_{33}\right]\right\} \\ D_{Bs}^m(A_{Bs}^m) &= D_p^m(A_{p\,\mathrm{ref}}^m) \left\{\sum_{n=0}^{8} W_n^m(A)\left|\tilde{D}_{Bs}^m(f_n^m)\right|^2\right\}^{-1} \times \\ &\left\{\frac{1}{2}\sum_{n=0}^{8} W_n^m(A)\,\tilde{D}_{Bs}^m(f_n^m)^*\left[R_{By}^m(A_{Bs}^m, f_n^m)\tilde{E}_{22} - R_{Bz}^m(A_{Bs}^m, f_n^m)\tilde{E}_{33}\right]\right\} \end{aligned} \tag{31}$$

where

$$\tilde{E}_{22} = \left(\tilde{S}_{Bs}^m(f_n^m) + \tilde{D}_{Bs}^m(f_n^m)\right) \quad \text{and} \quad \tilde{E}_{33} = \left(\tilde{S}_{Bs}^m(f_n^m) - \tilde{D}_{Bs}^m(f_n^m)\right) . \tag{32}$$

In each of these equations the two expressions in curly brackets are equal (and therefore cancel) when $A_{Bs}^m = A_{Bs\,\mathrm{ref}}^m$, as required by the calibration model.

We note that $\tilde{E}_{22}$ and $\tilde{E}_{33}$ may be expressed rather simply in terms eq. 24,

$$\tilde{E}_{22} = \sqrt{N_{22}^{mn}}\, e_2 \quad \text{and} \quad \tilde{E}_{33} = \sqrt{N_{33}^{mn}}\, e_3 \quad \text{for input noise density } \rho_{Bs\,\mathrm{ref}}^m . \tag{33}$$

These results are sumarised in Section 5.

4.5 Correction for the Sensor Transfer Functions

Most calibration signals are not injected at the level of the physical parameter which is being determined, *i.e.*, in the form of a magnetic or an electric field. Therefore, once the calibration coefficients have been determined as explained in the preceding section, the different parameters must be "corrected" for the transfer functions of the five sensors.

A complete correction is not possible. The calibration of STAFF-SA has been performed using noise signals, the calibration of the sensors is performed using analytic signals. Eq. 17 of the calibration procedure takes account of the passband of the AGC, and eq. 24 that of the digital filter. The data available for the sensors is in the form of the transfer function as a function of frequency; the best that can be done is to use the mean values obtained by integrating this transfer function over the different passbands.

Note that different lengths for the E_y and the E_z antennas enter into the category of differences of sensor transfer function which must be handled using the equations derived below.

Let $U_i(f)$ be the five sensor transfer function, so that the fifteen overall "receiver + sensor" transfer functions are (*Label* **corF**)

$$F_i'^m(f, A_i^m) = U_i(f)\ F_i^m(f, A_i^m)\ . \tag{34}$$

To represent the effects of the sensors on the calibration coefficients, we calculate

$$U_i^m = \frac{\int_{-\infty}^{\infty} U_i(f)\, G^m(f)\, df}{\int_{-\infty}^{\infty} G^m(f)\, df}$$

where $G^m(f)$ is the analogue receiver AGC passband characteristic for band m, and

$$u_i^{mn} = \frac{\int_{-\infty}^{\infty} U_i(f)\, B^{mn}(f)\, df}{\int_{-\infty}^{\infty} B^{mn}(f)\, df}$$

where B^{mn} is the digital analyser passband characteristic introduced in Sect. ref. 21 of Appendix 1. To determine the coefficients u_i^{mn} it is adequate to take "spot values" at each of the 27 central frequencies of the digital filter; but to evaluate the U^m the sensor transfer function must be integrated over the width of the AGC bandwidth function $G^m(f)$. Note that the precision of the evaluation of U^m need not be very great, as it effectively enters only into the determination of $S_p^m(A_p^m)$, which is used only for the evaluation, via eq. defSQ, of the spectral noise density in a rather wide band.

4.5.1 The functions $S_p'^m(A_p^m)$ and $D_p'^m(A_p^m)$

The function $S_p'^m(A_p^m)$ must be defined by eq. 17. From knowledge of the spin-plane AGC circuit, the effect of the spin-plane sensor transfer functions on the AGC value A_p^m (and hence on $S_p^m(A_p^m)$) is approximately equivalent to replacing ρ by $\rho \times \sqrt{|U_{py}^m|^2 + |U_{pz}^m|^2}$. It is convenient to define (*Label* **defV**)

$$V_{Bx}^m = |U_{Bx}^m|\ , \qquad V_{Bs}^m = \sqrt{\frac{|U_{By}^m|^2 + |U_{Bz}^m|^2}{2}}\ , \qquad V_{Es}^m = \sqrt{\frac{|U_{Ey}^m|^2 + |U_{Ez}^m|^2}{2}}\ . \tag{35}$$

Then, to maintain the validity of eq. 17, the modified functions $S_p^m(A_p^m)$ are

$$S_p'^m(A_p^m) = \frac{S_p^m(A_p^m)}{V_p^m}\ , \tag{36}$$

while to maintain the validity of eq. 23

$$D_p'^m(A_p^m) = \frac{D_p^m(A_p^m)}{V_p^m}\ . \tag{37}$$

Note that, since the sensor transfer functions $U_i(f)$ are independent of signal amplitude, the phase of the functions $S_p^m(A_p^m)$ and $D_p^m(A_p^m)$ is unchanged by the sensors. (This is fortunate, because the determination of these phases is itself not very clear, see Sect. 4.4.2.)

4.5.2 The coefficients $\tilde{S}_p'^n$ and $\tilde{D}_p'^n$

The phase differences introduced by the sensor transfer functions are reflected in the coefficients $\tilde{S}_{Bs}'^{mn}$ and $\tilde{S}_{Bs}'^{mn}$, as are amplitude variations between different channels within the same band m.

Eqs. 2, 3 and 34 may be used to obtain, using the spin-plane magnetic field as example,

$$\begin{aligned}
\mathcal{S}'^n_{Bs} &= \frac{1}{2}\left[\left(u^n_{By} + u^n_{Bz}\right)\mathcal{S}^n_{Bs} + \left(u^n_{By} - u^n_{Bz}\right)\mathcal{D}^n_{Bs}\right] \\
\mathcal{D}'^n_{Bs} &= \frac{1}{2}\left[\left(u^n_{By} - u^n_{Bz}\right)\mathcal{S}^n_{Bs} + \left(u^n_{By} + u^n_{Bz}\right)\mathcal{D}^n_{Bs}\right]
\end{aligned}$$

Substituting from eq. 3,

$$\begin{aligned}
S'_{Bs}\tilde{S}'^n_{Bs} &= \frac{1}{2}\left[\left(u^n_{By} + u^n_{Bz}\right)S_{Bs}\tilde{S}^n_{Bs} + \left(u^n_{By} - u^n_{Bz}\right)D_{Bs}\tilde{D}^n_{Bs}\right] \\
D'_{Bs}\tilde{D}'^n_{Bs} &= \frac{1}{2}\left[\left(u^n_{By} - u^n_{Bz}\right)S_{Bs}\tilde{S}^n_{Bs} + \left(u^n_{By} + u^n_{Bz}\right)D_{Bs}\tilde{D}^n_{Bs}\right]
\end{aligned}$$

Using the values of $S'^m_p(A^m_p)$ and $S'^m_p(A^m_p)$ from eqs. 36 and 37

$$\left.\begin{aligned}
\tilde{S}'^n_p &= \tfrac{1}{2}V^m_p\left[\left(u^n_{py} + u^n_{pz}\right)\tilde{S}^n_p + \left(u^n_{py} - u^n_{pz}\right)\tilde{D}^n_p\right] \\
\tilde{D}'^n_p &= \tfrac{1}{2}V^m_p\left[\left(u^n_{py} - u^n_{pz}\right)\tilde{S}^n_p + \left(u^n_{py} + u^n_{pz}\right)\tilde{D}^n_p\right]
\end{aligned}\right\}\quad \text{for } p = 2, 3\ . \tag{38}$$

The axial component is much simpler: using analogous notation,

$$\tilde{S}'^n_p = V^m_p\, u^n_{px}\, \tilde{S}^n_p \quad \text{for } p = 1\ . \tag{39}$$

The reason for the factor V^m_p appearing in these equations is simply to offset the same factor appearing in the denominator of equations 36 and 37. This why the output from the digital spectrum analyser can be reliably converted to physical units even if the evaluation of U^m_i (eq. 4.5) is only rather approximate.

5 Discussion

Eqs. 31 enable $S^m_{Bs}(A^m_{Bs})$ and $D^m_{Bs}(A^m_{Bs})$ to be determined in terms of :

- $R^m_{By}(A^m_{Bs}, f^m_n)$ and $R^m_{Bz}(A^m_{Bs}, f^m_n)$; these quantities are measurable, as explained in Section 4.4.1. Furthermore, these functions describe **completely** (magnitude and phase) the variation of the receiver transfer function with both AGC level A^m_p and channel frequency f^m_n.
- $\tilde{E}_{22}$ and $\tilde{E}_{33}$, which are related by eq. 33 to $\sqrt{N^{mn}_{22}}e_2$ and $\sqrt{N^{mn}_{33}}e_3$, quantities determined at the reference level $\rho^m_{Bs;\mathrm{ref}}$, as explained in Section 4.3.3.
- $\tilde{S}^m_{Bs}(f^m_n)$ and $\tilde{D}^m_{Bs}(f^m_n)$, which are simply linear combinations of $\tilde{E}_{22}$ and $\tilde{E}_{33}$ (see eq. 24, equivalent to eqs. 32 and 33).
- $W^m_n(A)$, a quality parameter determined in Section 4.3.3 using the method of Section 3.2.

A number of observations can be made.

1. Applied separately for all 256 values of A (that is, 256×3 values of $m \times 2$ values of $p = 1536$ values of A^m_p *per satellite*), eqs. 31 determine the functions $S(A)$ and $D(A)$ completely (in magnitude and phase). In reality, the measurements will not be done for all 256 possible values of A, but only at a limited number of values of the input noise level. It should be noted that, in principle, the functions $S(A)$ and $D(A)$ vary smoothly with A ; therefore if the measurements are performed for values of A which are sufficiently close, some smoothing may be performed to reduce the experimental errors. Finally, interpolation will be used to obtain these functions for all 256 possible values of A, as required for the calibration model.
2. All nine frequency channels (values of n) are used for the determination of each value of $S(A)$ and $D(A)$, wieghted by the quality factor $W(A)$ determined from the mutual redundancy of the 10 cross-correlation factors via eq. 13 (page 7). Some channels may be contaminated by interference ; because the interference is phase coherent (*e.g.*, at 50 Hz), eq. 13 will yield a particularly good quality factor $W^m_n(A)$ at these frequencies. For these values of m and n, $W^m_n(A)$ must be set manually to zero for all values of A.
3. It can be seen that the choice of the nine reference input noise levels $\rho^m_{p\,\mathrm{ref}}$ as described in Section 4.3.1 may need to be revised. For example, there is clearly a mathematical problem if the receivers are perfectly balanced so that $\tilde{D}(f^m_n) = 0$ for all n. This is real physical problem : the model is based upon eq. 3, so that if $\tilde{D}(f^m_n) = 0$ when $A^m_p = A^m_{p\,\mathrm{ref}}$, it is totally incapable of taking account of any values $\tilde{D}(f^m_n) \neq 0$ when $A^m_p \neq A^m_{p\,\mathrm{ref}}$. Finally, the choice of $\rho^m_{p\,\mathrm{ref}}$ is rather delicate.
4. To avoid this problem, it may be possible to generalise the method of Sect. 4.4.2 so as to determine by the method of least squares the coefficients $S^m_p(A^m_p)$ and $D^m_p(A^m_p)$ (representing the variation with AGC of the magnitude and phase of the gain) simultaneously with the coefficients $\tilde{S}^m_p(f^m_n)$ and $\tilde{D}^m_p(f^m_n)$ (representing the variation with frequency of the magnitude and phase of the gain). This necessitates the solution of $2 \times 256 + 9 = 521$ simultaneous equations for each of the $3 \times 5 = 15$ receivers. This daunting task has not been attempted ; beforehand, the stability of the resulting solution (with respect to experimental errors, interference, *etc.*) must be examined.

APPENDIX 1

Cross-References to Technical Note TN-0001

The calibration tables used in this document are described in the document "Conversion of the Science Data to Physical Units", ref. OBSPM–TN–0001, to which frequent reference is made.

To handle semi-automatically the equation numbering in the two documents through successive revisions, the following table is generated from a file which is common to both papers. The numbers in the first column, as well as the description of the item, are common to this appendix and the corresponding appendix at the end of paper OBSPM–TN–0001.

Ref 1. X_i is expressed in terms of x_i by in Paper TN–0001

Ref 2. The relation between F, P and Q in Paper TN–0001

Ref 3. The De-Spin Algorithm in Paper TN–0001

Ref 4. The sum and difference functions are defined in Paper TN–0001

Ref 5. The sum and difference noise functions are defined in Paper TN–0001

Ref 6. The separation of the spin-plane variables is described in Paper TN–0001

Ref 7. The equation separating the variables for $\mathcal{S}$ and $\mathcal{D}$ is in Paper TN–0001

Ref 8. The equation to redefine F, P and Q is in Paper TN–0001

Ref 9. The overall (analogue + digital) receiver response is given in Paper TN–0001

Ref 10. The matrix Δ_{ij} is defined in Paper TN–0001

Ref 11. The small parameters ϵ_p^m are defined in Paper TN–0001

Ref 12. The indices p and q are determined in Paper TN–0001

Ref 13. The Physical Significance of $S_p^m(A_p^m)$ and $\tilde{S}_p^m(f^n)$ in Paper TN–0001

Ref 14. The Complete Set of Calibration Coefficients is described in Paper TN–0001

Ref 15. The definition of Q in Paper TN–0001

Ref 16. The relation between N_{ij}^n and $< \overline{X}_i \overline{X}_j^* >$ is in Paper TN–0001

Ref 17. The expression for $< \overline{X}_i \overline{X}_j^* >$ when the despin is OFF is in Paper TN–0001

Ref 18. The non-diagonal elements are normalised in Paper TN–0001

Ref 19. The two options for separating the variables are compared in Paper TN–0001

Ref 20. The computation of Δ_ij is detailed in Paper TN–0001

Ref 21. The digital receiver spectral passband characteristic is introduced in Paper TN–0001

Ref 22. Figure 1 of TN–0001 in Paper TN–0001

Ref 23. Section "The axial component B_x" in Paper TN–0001

Ref 24. Relation to determine Q^m_{Bx} in Paper TN–0001

Ref 25. Section "The phase of the Q^m_i functions" in Paper TN–0001

Ref 26. Section "Logarithmic decompression of the digital output" in Paper TN–0001

Ref 27. The expression for N_{ij} in terms of $< \overline{x}_i \overline{x}^*_j >$ is given in Paper TN–0001

APPENDIX 2

Determination of the Phase Calibration

If the absolute phases of the five channels are represented by the e_i with $|e_i| = 1$, then the relative phase between channel i and channel j is $e_i e_j^*$. All the different pairs of relative phases may be represented by the matrix $e_i e_j^*$. On the other hand, experimental noise between the channels will be non-correlated, and the associated correlation matrix will be diagonal, $e_i e_j^* = \delta_{ij}$. Now, any 5×5 Hermitian matrix can be expressed in terms of its eigenvalues and eigenvectors, thus:

$$C_{ij} = \sum_{\lambda=1}^{5} \lambda^{(\lambda)} u_i^{(\lambda)} u_j^{*(\lambda)}$$

where $u_i^{(\lambda)}$ is the eigenvector corresponding to the eigenvalue $\lambda^{(\lambda)}$. Thus the information content of the eigenvalues and eigenvectors is identical to that of C_{ij}. In the reference frame defined by its eigenvectors, the matrix is diagonal,

$$C_{ij} = \begin{pmatrix} \lambda^{(1)} & 0 & 0 & 0 & 0 \\ 0 & \lambda^{(2)} & 0 & 0 & 0 \\ 0 & 0 & \lambda^{(3)} & 0 & 0 \\ 0 & 0 & 0 & \lambda^{(4)} & 0 \\ 0 & 0 & 0 & 0 & \lambda^{(5)} \end{pmatrix} .$$

For a pure signal C_{ij} would have only one non-zero eigenvalue. In the general case, let the eigenvalues be ordered $\lambda^{(1)} \leq \lambda^{(2)} \leq \lambda^{(3)} \leq \lambda^{(4)} \leq \lambda^{(5)}$. Then C_{ij} may be expressed

$$\begin{aligned} C_{ij} \;=\; & \lambda^{(1)} \begin{pmatrix} 1 & 0 & 0 & 0 & 0 \\ 0 & 1 & 0 & 0 & 0 \\ 0 & 0 & 1 & 0 & 0 \\ 0 & 0 & 0 & 1 & 0 \\ 0 & 0 & 0 & 0 & 1 \end{pmatrix} \\ & + (\lambda^{(2)} - \lambda^{(1)}) \begin{pmatrix} 0 & 0 & 0 & 0 & 0 \\ 0 & 1 & 0 & 0 & 0 \\ 0 & 0 & 1 & 0 & 0 \\ 0 & 0 & 0 & 1 & 0 \\ 0 & 0 & 0 & 0 & 1 \end{pmatrix} + (\lambda^{(3)} - \lambda^{(2)}) \begin{pmatrix} 0 & 0 & 0 & 0 & 0 \\ 0 & 0 & 0 & 0 & 0 \\ 0 & 0 & 1 & 0 & 0 \\ 0 & 0 & 0 & 1 & 0 \\ 0 & 0 & 0 & 0 & 1 \end{pmatrix} \\ & + (\lambda^{(4)} - \lambda^{(3)}) \begin{pmatrix} 0 & 0 & 0 & 0 & 0 \\ 0 & 0 & 0 & 0 & 0 \\ 0 & 0 & 0 & 0 & 0 \\ 0 & 0 & 0 & 1 & 0 \\ 0 & 0 & 0 & 0 & 1 \end{pmatrix} + (\lambda^{(5)} - \lambda^{(4)}) \begin{pmatrix} 0 & 0 & 0 & 0 & 0 \\ 0 & 0 & 0 & 0 & 0 \\ 0 & 0 & 0 & 0 & 0 \\ 0 & 0 & 0 & 0 & 0 \\ 0 & 0 & 0 & 0 & 1 \end{pmatrix} . \end{aligned}$$

The first term is the contribution from fully isotropic uncorrelated noise, and the last term is the contribution from a fully coherent (*i.e.*, the calibration) signal. The proportion of the power in the fully polarised wave (the signal to noise ratio) is

$$P = \frac{\lambda^{(5)}}{\lambda^{(1)} + \lambda^{(2)} + \lambda^{(3)} + \lambda^{(4)} + \lambda^{(5)}} . \tag{40}$$

P lies in the range $\frac{1}{5} \leq P \leq 1$, with $P = 1$ corresponding to no noise. Hopefully $\lambda^{(1)} \simeq \lambda^{(2)} \simeq \lambda^{(3)} \simeq \lambda^{(4)}$: if this is not the case, further investigation will be required. An effect of this type may be introduced by systematic errors in the calibration analysis results arising from the course granularity of the quantisation of the off-diagonal elements of the cross-spectral matrix; but this is pure speculation at the present time.